

CFD MODELLING OF LIQUID JET AND CASCADE BREAKUP IN CROSSFLOWS

Benny KUAN

Process Science and Engineering, Commonwealth Scientific and Industrial Research Organisation
Box 312, Clayton South, VIC 3169, AUSTRALIA

ABSTRACT

Formation and breakup of liquid droplets play key roles in a wide range of chemical processes, most of which are concerned with atomising the liquid into fine droplet sprays in a co-flow environment where the liquid jet is sandwiched between high-velocity air streams to produce a droplet cloud. The present work deals with droplet breakup in a cross-flow environment where the air stream directly impacts onto a liquid jet or column. A CFD model has been developed for the breakup of this liquid jet and subsequent formation of droplets. The model has been tested for liquid jets in a crossflow that are documented in the published literature. Both the shape of the liquid column and dispersion pattern of the droplets as predicted by the model agree well with the published data.

NOMENCLATURE

C	model constant
C_D	drag coefficient
d	droplet diameter
\mathbf{F}	momentum source
k	turbulence kinetic energy
M	Mach number
n	droplet number density
On	Ohnesorge number
P	pressure
q	liquid/air momentum flux ratio, $\rho_l v_f^2 / \rho_a v_a^2$
r	volume fraction
T	characteristic timescale for droplet breakage
\mathbf{U}	mean velocity vector
\mathbf{u}'	fluctuating velocity vector
V_{slip}	slip velocity
w	cascade width
We	Weber number
α	phase
ε	turbulence dissipation rate
ρ	density
σ	Prandtl number
μ	dynamic molecular viscosity

INTRODUCTION

Formation and breakup of liquid droplets play key roles in a wide range of chemical processes, including fuel spray in combustors, spray coating, powder formation, and gas scrubbing. Most of these processes are concerned with atomising the liquid into fine droplet sprays in a co-flow environment in which the liquid jet is sandwiched between high-velocity air streams to produce a droplet cloud. There is a large body of scientific knowledge addressing this topic (Varga et. al., 2003; Inamura and Daikoku, 2002; Park et. al. 2002) in the published literature.

By comparison, liquid droplets used in some industrial processes, such as spray cooling towers, need to be introduced in such a way that facilitates maximum contact between a large body of gas and the liquid. In cases where the gas temperature is considerably less than boiling point of the liquid, liquid droplets can be sprayed directly onto the gas to strip the solids off the particle-laden gas stream. However, for processes where the liquid also plays a significant role in cooling the gas through vaporisation, it is not appropriate to spray fine liquid droplets onto the hot gas streams. Liquid droplets thus need to be generated using an opposing- or cross-flow arrangement with respect to the gas stream.

Wu et. al. (1995, 1997, 1998) have performed a series of experiments to examine the atomisation of an upflowing liquid jet injected into a strong crossflow. Parameters investigated include liquid injection velocity, gas velocity and liquid surface tension. Their flow visualisation study has revealed a series of events taking place during the liquid jet breakup process. Breakup first starts at the liquid jet surface from which some liquid fragments are stripped and droplets form. This causes instability to the jet surface in the form of acceleration waves which deform and flatten the liquid column. The liquid column eventually disintegrates into ligaments and droplets.

The present paper outlines the development of a droplet breakup model that is suitable for Eulerian-Eulerian two-phase flow applications where the particle phase is solved as a continuum fluid. The model is based on a population-balance approach with one governing equation representing the transport of droplet number density. Droplet breakup is evaluated based on local droplet Weber number and reflected as a source term to the population-balance equation. The model is validated using experimental data provided in Wu et. al. (1997) and Lim et. al. (2006). Model development and results of model validation are presented in this paper.

MODEL DESCRIPTION

Gas and liquid flow models were developed using a commercial CFD code ANSYS CFX-11 and are based on a two-fluid approach. The flow field is assumed to be in a steady-state throughout the flow domain.

Two-Fluid Model

Gas and liquid flow properties are calculated by numerically solving the following set of Reynolds-averaged Navier-Stokes equations for each phase α

$$\nabla \cdot (r_\alpha \rho_\alpha \mathbf{U}_\alpha) = 0 \quad (1)$$

$$\begin{aligned} \nabla \cdot (r_\alpha \rho_\alpha \mathbf{U}_\alpha \mathbf{U}_\alpha) &= -r_\alpha \nabla P_\alpha \\ &+ \nabla \cdot (r_\alpha \mu_\alpha \nabla \mathbf{U}_\alpha) \\ &- \nabla \cdot (r_\alpha \rho_\alpha \overline{\mathbf{u}'_\alpha \mathbf{u}'_\alpha}) + \mathbf{F}_h \end{aligned} \quad (2)$$

where $\overline{\mathbf{u}'_\alpha \mathbf{u}'_\alpha}$ is Reynolds stresses. The momentum source term, \mathbf{F}_h , takes into account hydrodynamic forces acting on the dispersed phase and the resulting interfacial forces on the continuous phase.

A $k-\varepsilon$ turbulence model, modified to account for two phase flow, is used in this study to account for the effect of turbulence in both the gas and liquid flow field. Eddy viscosity $\mu_{t\alpha}$ for phase α is defined as

$$\mu_{t\alpha} = \begin{cases} C_\mu \rho_\alpha k^2 / \varepsilon, & \alpha = \text{gas} \\ \frac{\rho_\alpha}{\rho_{\text{gas}}} \frac{\mu_{t,\text{gas}}}{\sigma_\alpha}, & \alpha = \text{liquid} \end{cases} \quad (3)$$

Solution of the governing equations is based on a finite volume approach with the advection terms approximated using a ‘‘High Resolution Scheme’’ which is second order accurate. Further details of the solution process are available in Ansys Inc. (2007).

Droplet Motion

Hydrodynamic Forces

In a two phase flow system consisting of a continuous gas phase and a dispersed liquid phase, the hydrodynamic force acting on the dispersed phase and its back-influence on the continuous phase can also critically affect gas and droplet motion. Such a dependency is modelled through \mathbf{F}_h which represents the combined effect of inter-phase drag, lift force, virtual mass force, gravity, and turbulent dispersion. Of all the hydrodynamic forces considered in the simulation, the inter-phase drag is the most important. The present simulation makes use of a drag model of Clift et al. (1978) which considers the effect of fluid droplet shape transition from a sphere at low droplet Reynolds number Re_p to an ellipsoid at high Re_p . In the model, droplet shape is characterised by Eotvos number Eo which, like Re_p , is also a function of the droplet size d_p . However, the droplet size d_p is not a constant and varies spatially throughout the flow domain. A reliable droplet size model is thus necessary to ensure the effect of inter-phase drag is adequately accounted for in the model.

Droplet Breakup

A droplet size model which reflects the formation and breakup of liquid droplets has been developed and it provides an estimate of the local liquid droplet size everywhere within the flow domain. In our model, the timescale of liquid droplet formation and breakup is determined from a breakup model which was originally proposed by Pilch and Erdman (1987) and later reviewed by Gelfand (1996). In their studies, the droplet breakup process is categorised into different regimes by droplet Weber number. Based on time history data collected from published experiments, such as Hassler (1970) and Li and Fogler (1978), Pilch and Erdman postulated the following correlations for total breakup time, ΔT

$$\Delta T = \beta \cdot T^* \quad (4)$$

$$T^* = \frac{d_p}{V_{\text{slip}}} \sqrt{\frac{\rho_p}{\rho_f}} \quad (5)$$

$$\beta = \begin{cases} 6(We - We_{\text{crit}})^{-0.25}, & We_{\text{crit}} < We \leq 18 \\ 2.45(We - We_{\text{crit}})^{0.25}, & 18 < We \leq 45 \\ 14.1(We - We_{\text{crit}})^{-0.25}, & 45 < We \leq 351 \\ 0.766(We - We_{\text{crit}})^{0.25}, & 351 < We \leq 2670 \\ 5.5, & 2670 < We \end{cases} \quad (6)$$

with We_{crit} being the critical Weber number.

Droplet size after total breakup is determined from a model of Schmehl et al. (2000) where

$$d_p^{(1)} = d_p^{(0)} f_{br} \quad (7)$$

with $d_p^{(0)}$ and $d_p^{(1)}$ respectively denote droplet diameter before and after droplet breakup;

$$f_{br} = 1.5 On^{0.2} We_{\text{corr}}^{-0.25} \quad (8)$$

$$On = \frac{\mu_p}{\sqrt{\rho_p d_p^0 \sigma}} \quad (9)$$

$$We = \frac{\rho_f V_{\text{slip}}^2 d_p^0}{\sigma} \quad (10)$$

$$We_{\text{corr}} = \frac{We}{1 + 1.077 On^{1.6}} \quad (11)$$

V_{slip} refers to slip velocity between gas and the droplets and σ is droplet surface tension coefficient.

Droplet Weber number, as defined in equation (10), is recognised as the single most important parameter that characterises droplet breakup in the literature (Wu et al., 1995 & 1997). It is a measure of disruptive hydrodynamic forces with respect to the stabilising surface tension force. Being a dimensionless parameter, one can expect a breakup model that is developed based on the droplet Weber number to be applicable to a wide range of gas-liquid flow systems.

In order to predict the variation of droplet size due to breakup within the flow domain, equations (4) and (7) are applied to construct a simplified population balance equation to model local growth of droplet population due to droplet breakup. The model tracks the droplet number density, n , using the equation

$$\nabla \cdot (r_l \rho_l \mathbf{U}_l n) = r_l \rho_l S_{br} \quad (12)$$

The source term S_{br} for equation (12) represents the time rate of change in droplet population per unit volume, i.e.

$$S_{br} = C \cdot \frac{n^{(1)} - n^{(0)}}{\Delta T} \quad (13)$$

with C being a model constant. Liquid droplets are assumed to remain intact where $We < We_{\text{crit}}$. The

associated S_{br} is thus set to zero to reflect negligible growth in local droplet numbers.

Droplet size is determined from droplet number density n through the following expression

$$n = \frac{r_p}{\frac{\pi}{6} d_p^3} \quad (14)$$

where r_p is volume occupied by the liquid phase in a control volume.

Boundary Conditions

Equation (12) allows one to control droplet breakup/growth through the definition of the source term S_{br} . The present study assumes that all wall surfaces are wetted and are covered by an established thin liquid film. Following the experimental observation of Pan and Law (2005) who have categorised typical regimes in which droplet-film absorption occurs, droplets that collide with a liquid film on top of a solid surface will either be deflected away or absorbed into the film depending on the normalised film thickness and droplet collision Weber number $We_{collision}$ which is calculated as a function of droplet impact velocity and liquid density.

Where the droplet-film collision results in droplet absorption into the film, the source term S_{br} at the wall is set to zero. The droplet number density is arbitrarily set to unity at all walls. Free-slip condition is assumed for the liquid phase at the wall surfaces and hence the effect of wall friction which acts to slow down liquid movement on the wall is not considered in the model.

At the liquid inlet, an initial droplet size is estimated from hydraulic diameter of the discharge slots. Following equation (14), this then leads to an approximated inlet droplet number density. For the gas inlet, the droplet number density is zero corresponding to zero liquid volume fraction.

For the liquid jet breakup, the computed flow domain covers a 3D region that is 40d tall, 50d long and 20d wide (ref. Figure 1). All faces of the flow domain are assumed to be free boundaries, except the bottom one which is a wall with a jet inlet. More than 270,000 elements were used.

For the liquid cascade breakup, the flow domain is $1w$ wide and stretches $4w$ and $2.4w$ in the streamwise and vertical directions (ref. Figure 5). All domain faces are set up as free boundaries, except the back face which is a solid wall and the front face through which the swirling jet enters the flow domain. More than 670,000 elements were used in the simulation.

MODEL VALIDATION

Liquid Jet Breakup in Crossflows

Experimental data obtained for the breakup of a vertically upward water jet as studied in Wu et. al. (1997) has been applied to validate the CFD model. In the experiment, a water jet with a diameter of 0.5 mm is injected upwards at 28 m/s into an air flow field which is dominated by a horizontal crossflow at Mach number $M = 0.2, 0.3$ and

0.4. Shadowgraphs of the water jets under the influence of the crossflow were generated from the experiment based on which Wu et al. (1997) proposed a correlation for the liquid column trajectories:

$$\frac{y}{dq} = \sqrt{\pi/C_D} \left(\frac{x}{dq} \right)^n \quad (15)$$

where d is jet diameter; q is liquid/air momentum flux ratio; (x, y) is the coordinate of the liquid column trajectory as sketched in Figure 1.

Their trajectory analysis for the water jet indicated a mean C_D value of 1.5 with standard deviation of 0.45, and $n = 0.5$. Water jet trajectories based on the numerical simulation for crossflow velocities of $M = 0.2, 0.3$ and 0.4 are compared against the experimental profiles in Figure 2. The CFD results presented in the figure are based on a critical Weber number of 80 and $C = 0.05$. The critical Weber number is set on the basis of Wu et al.'s experimental observation. The predicted water jet trajectories for all crossflow velocities fall within one standard variation of the mean profile.

Success of the present modelling approach lies in the fact that the droplet Weber number is high at the base of the liquid column ($We = 77$ for $M = 0.2$) such that the breakup is dominated by a process similar to that of the secondary breakup of a spherical droplet.

The model, however, is unable to capture fracture of the liquid column as observed in the experiment. According to Wu et. al., upon introduction of the liquid jet into the air crossflow, the liquid column first undergoes surface breakup in which some droplets are stripped from the column surfaces. The remainder of the liquid column then deforms under the action of aerodynamic forces and eventually disintegrates into ligaments and droplets.

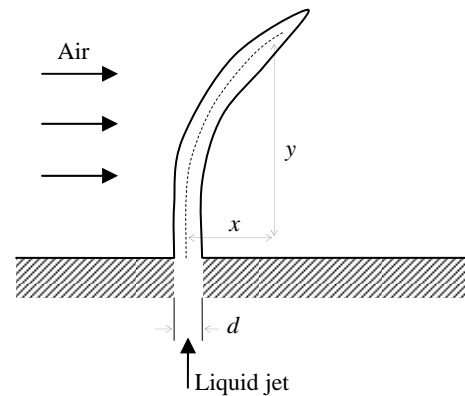


Figure 1: Sketch of the liquid column trajectory.

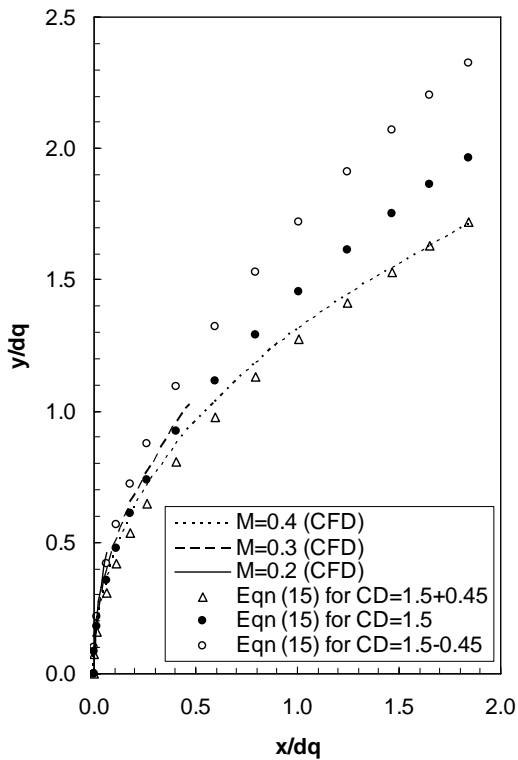


Figure 2: Comparison of water jet trajectories.

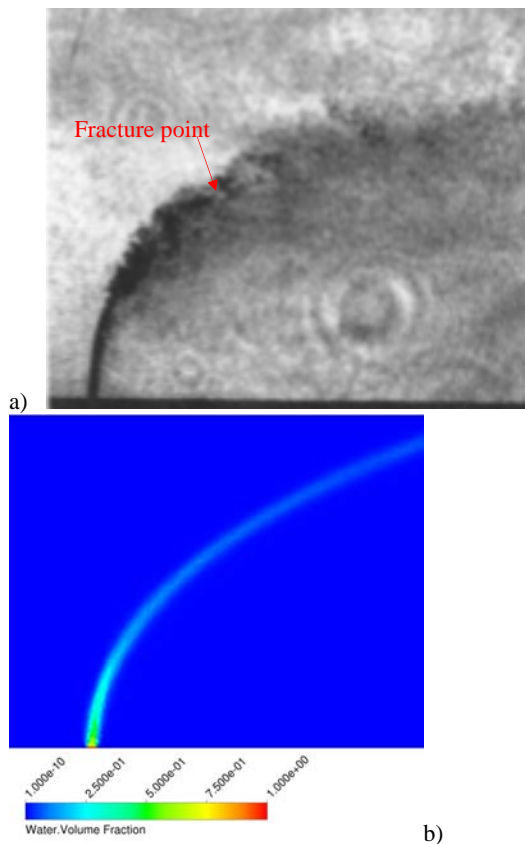


Figure 3: Comparison of water column profiles distribution. a) shadow graph extracted from Wu et. al. (1997); b) predicted water volume fraction on centre-plane.

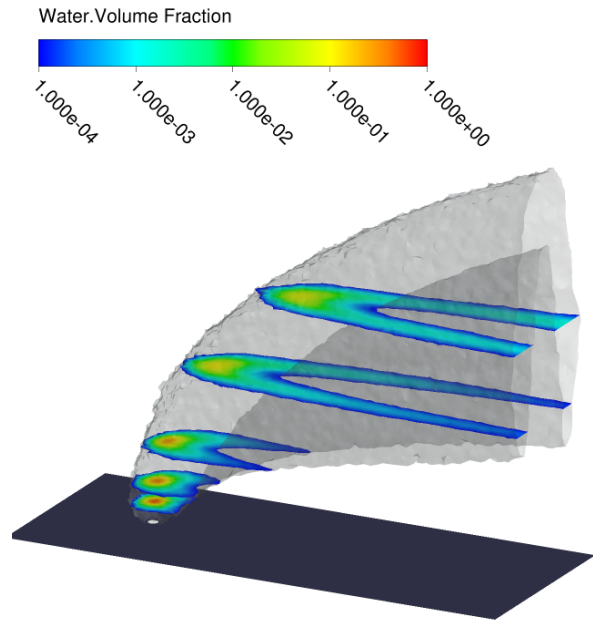


Figure 4: Three-dimensional structure of the water jet at $M = 0.4$.

A shadow graph extracted from Wu et. al. (1997) for water jet in air crossflow at $M = 0.4$ is compared against the predicted centre-plane distribution of water volume fraction in Figure 3. In the experiment, column fracture location is identified by a discontinuity in the water column. This point is marked in Figure 3a). By comparison, the prediction indicates a gradual decay of water volume fraction as a direct result of droplet breakup.

Despite the above weakness, the model does provide a realistic representation on water column breakup. Iso-surface plots for water volume fraction over $1.0E-4$ are presented in Figure 4. Cross-section of the water column is found to be in the shape of a horseshoe. This correlates well with the findings of Cavaliere et al. (2003) who utilised a laser light scattering technique to reconstruct the cross-sectional shape of a liquid jet spray at high pressure. A 'kidney' shaped spray cross-section was observed. One can thus expect the side view of the water column in Figure 4 to match with the shape of the deformed water column as seen in the shadowgraph (Figure 3a).

Breakup of Liquid Cascade

Lim et. al. (2006) has performed a flow visualisation study on the breakup of liquid cascading from the edge of a steel roof. This is sketched in Figure 5. As shown in the figure, a swirling nozzle is placed at a horizontal distance L and vertical distance H from the edge of the roof. The nozzle is directed at the water cascade running from the edge of the roof.

It is hypothesised in the present study that an infinite number of liquid columns form the liquid cascade which disintegrates into droplets. The CFD model as developed previously has been applied to simulate the breakup of the liquid cascade. Computations were performed for air jet velocity ranging between 0 and 30 m/s. Some of the modelling results are presented in Figure 6.

Figure 6 plots the predicted centre-plane distribution of water volume fraction at increasing gas jet velocities. At

0 m/s, water cascades from leading and trailing edges of the roof under the influence of gravity (Figure 6a). An increase in the air jet velocity brings distortion to the water columns through the action of gas-liquid entrainment. At 30 m/s (Figure 6d), the gas jet is strong enough to completely entrain the water columns, thus

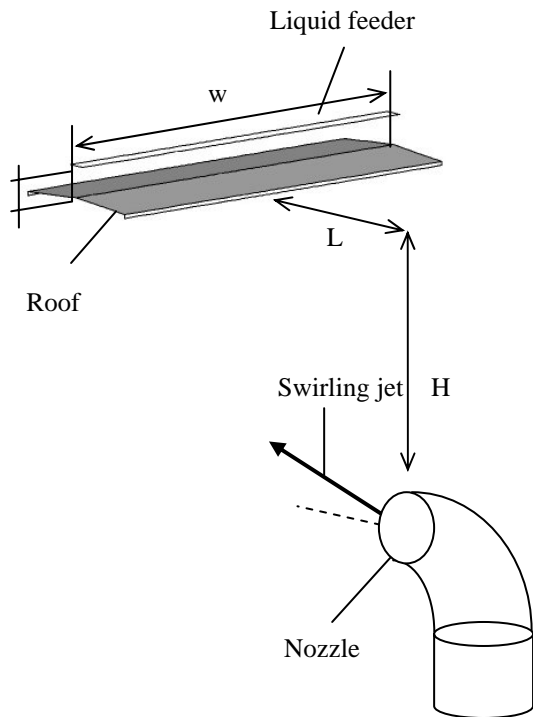


Figure 5: Sketch of the liquid cascade test rig

producing a longer and more visible water trail in the downstream direction.

As shown in Figure 6b and 6c, droplet breakup is more pronounced underneath the trailing edge. This is due to gas jet spreading underneath the influence of swirl such that the jet entrains a larger body of air further away from the nozzle. Therefore, whilst the slip between the two phases is very strong but localised in the leading columns, the gas-liquid slip in the trailing columns is weaker but more extensive and yet sufficient to cause droplet breakup. At 30 m/s (Figure 6d), the air jet essentially blows all liquid columns in the direction of the jet.

Distribution and movement of the water columns are found to match well with the experimental observation.

Water streamlines are plotted in FIGURE 7. The water streamlines serve to represent water columns cascading down the roof at gas jet velocities of 10 and 30 m/s. FIGURE 7a indicates local penetration of the gas jet through the water columns (10 m/s case) while the gas jet pertaining to the 30 m/s case has lifted both the front and rear water columns (FIGURE 7b). Apart from entraining the liquid columns in the direction of the gas jet, the gas jet also imparts swirling motion onto the liquid columns. Subsequently, centre-plane liquid columns are forced to veer away from the centre plane by the swirling gas jet, leading to seemingly weaker and shorter liquid streams at the trailing edge as seen in Figure 6b and c.

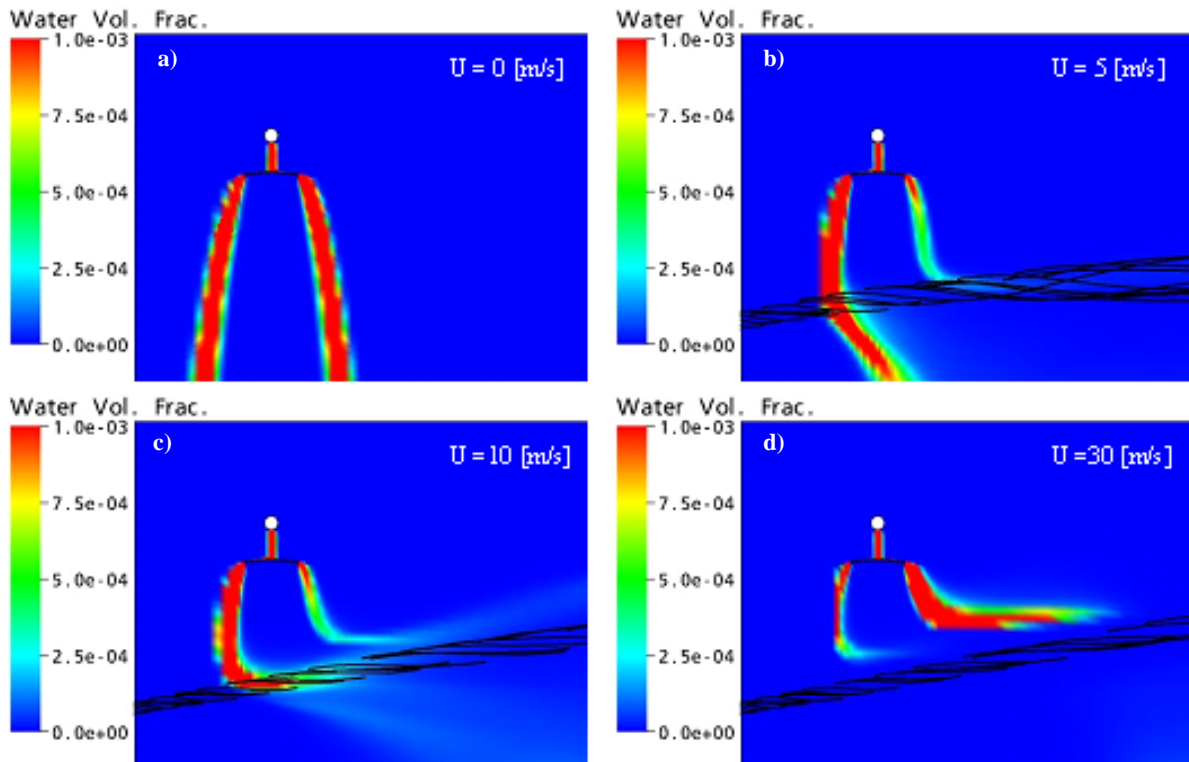


Figure 6: Predicted centre-plane distributions of water volume fraction at increasing jet velocity U . a) $U = 0$ m/s; b) $U = 5$ m/s; c) $U = 10$ m/s; d) $U = 30$ m/s.

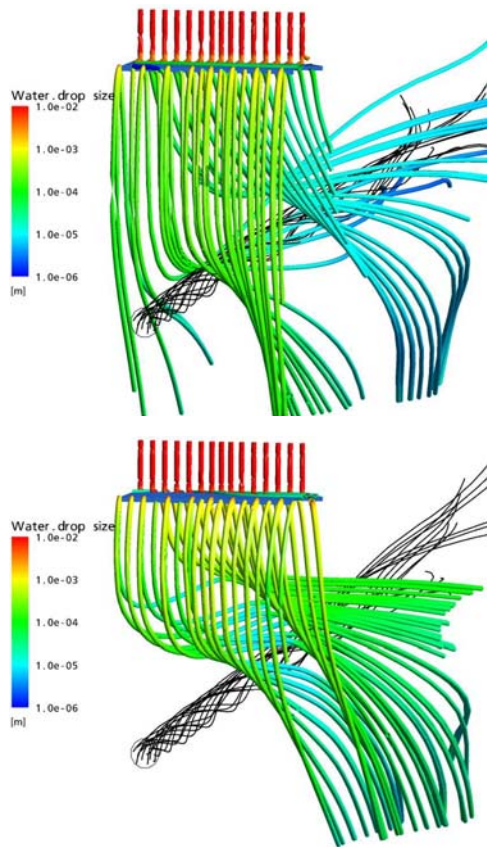


Figure 7: Predicted water streamlines under the influence of the gas jet (upper: $u = 10$ m/s; lower: $u = 30$ m/s)

CONCLUSION

An Eulerian-Eulerian two-phase model has been developed in an effort to capture the breakup process of liquid jets or columns. The model makes use of a modified scalar transport equation to account for droplet breakup as well as transport of droplets. Model validation has been performed for two crossflow cases where either a liquid jet or a liquid cascade is interrupted by a high speed air jet.

The model is able to realistically predict the deformation of both a liquid jet and cascade under the influence of a strong air jet in a crossflow arrangement. Further, the model has demonstrated its ability to capture the phenomenon of surface breakup reasonably well.

A major weakness of the model, however, lies in its poor representation of the free surface interfaces such that the shape of the liquid column is not well preserved in areas where droplet breakup is minimal, e.g. at the base of the column, or in areas where the column has terminated completely, e.g. column fracture.

Owing to a lack of particle size distribution data, size of the droplets produced during the modelled breakup process can not be directly verified.

REFERENCES

VARGA, C.M., LASHERAS, J.C. and HOPFINGER, E. J., (2003), "Initial breakup of a small-diameter liquid

jet by a high-speed gas stream", *J. Fluid Mech.*, **497**, 405-434.

INAMURA, T. and DAIKOKU M., (2002), "Numerical simulation of droplet formation from coaxial twin-fluid atomizer", *Atomization and Sprays*, **12**, 247-266.

PARK, J.W., HUH, K.Y., LI, X., and RENKSIZBULUT, M., (2002), "Experimental study on the breakup mechanism of a thin liquid sheet from an air-assisted planar nozzle", *J. Flow Visualization & Image Processing*, **9**, 257-270.

WU, P.K., MIRANDA, R.F., and FAETH, G.M., (1995), "Effects of initial flow conditions on primary breakup of nonturbulent and turbulent round liquid jets", *Atomization and Sprays*, **5**, 175-196.

WU, P.K., KIRKENDALL, K.A., FULLER, R.P., and NEJAD, A.S., (1997), "Breakup processes of liquid jets in subsonic crossflows", *J. Propulsion and Power*, **13**, 64-73.

WU, P.K., KIRKENDALL, K.A., FULLER, R.P. and NEJAD, A.S., (1998), "Spray structures of liquid jets atomized in subsonic crossflows", *J. of Propulsion and Power*, **14**, 173-182.

LIM, S., SANDERSON, J., DENKE, R., JOYCE, T., and SANETIS, S., (2006), Visualisation of Liquid Break-Up by Swirling Gas Jet from a Cyclone Gas Outlet Snout. CSIRO Minerals DMR-3013, Australia.

ANSYS INC, A., (2007), *ANSYS-CFX Version 11.0 Documentation*. Pittsburgh, Pennsylvania, United States of America.

CLIFT, R., GRACE, J.R., and WEBER M.E., (1978), *Bubbles, Drops and Particles*, Academic Press, New York, United States of America.

PILCH, M. and ERDMAN, C.A., (1987), "Use of Breakup time data and velocity history data to predict the maximum size of stable fragments for acceleration-induced breakup of a liquid drop", *Int. J. Multiphase Flow*, **13**(6), 741-757.

GELFAND, B.E., (1996), "Droplet breakup phenomena in flows with velocity lag", *Progress in Energy and Combustion Science*, **22**, 201-265.

HASSLER, G., (1970), "Breakup of large water drops under the influence of aerodynamic forces in a steady stream of stream and stream at subsonic velocities", *Proceedings of the 3rd International Conference on Rain Erosion and Related Phenomena*, Hampshire, England.

LI, M.K. and FOGLER, H.S., (1978), "Acoustic emulsification. Part 2. breakup of the large primary oil droplets in water medium", *J. Fluid Mechanics*, **88**, 513-528.

SCHMEHL, R., MAIER, G., and WITTIG, S., (2000), "CFD analysis of fuel atomization, secondary droplet breakup and spray dispersion in the premix duct of a LPP combustor", *Proceedings of 8th International Conference on Liquid Atomization and Spray Systems*, Pasadena, California, United States of America.

PAN, K.L. and LAW, C.K., (2005), "Dynamics of droplet film collision", *43rd AIAA Aerospace Science Meeting & Exhibition*, Reno, USA, Paper Number AIAA-2005-0352.

CAVALIERE, A., RAGUCCI, R., and NOVIELLO, C., (2003), "Bending and break-up of a liquid jet in a high pressure airflow", *Experimental Thermal and Fluid Science*, **27**, 449-454.